Vol 12 No 10, October 2003
1009-1963/2003/12(10)/1143-06

Chinese Physics

© 2003 Chin. Phys. Soc.
and IOP Publishing Ltd

Effects of matrices on Mie scattering in the mid-infrared region*

Liu Xiao-Dong(刘晓东)[a)b)], Li Shu-Guang(李曙光)[c)], Guo Hong-Lian(郭红莲)[a)], Zhang Dao-Zhong(张道中)[a)], Li Zhao-Lin(李兆霖)[a)], and Hou Lan-Tian(侯蓝田)[c)]

[a)] *Laboratory of Optical Physics, Institute of Physics, Chinese Academy of Sciences, Beijing* 100080, *China*
[b)] *Department of Electromechanical and Information Engineering, Dalian Nationality University, Dalian* 116600, *China*
[c)] *Institute of Infrared Optical Fibres and Sensors, Yanshan University, Qinhuangdao* 066004, *China*

(Received 9 September 2002; revised manuscript received 11 April 2003)

Various Mie scattering systems, each having a transparent matrix, are studied in the mid-infrared region. Our three theoretical scattering systems correspond to a lossless scatterer, an anomalous dispersive dielectric scatterer and a metal scatterer, each in a non-air usual matrix. The refractive-index effects of the matrix on scattering and extinction efficiencies in the mid-infrared region are found to be quite different in different cases. Although the non-air usual matrix reduces scattering and extinction efficiencies in the first kind of system, it may or may not help scatter and extinguish the mid-infrared radiation in the second, and it has little effect on them in the third.

Keywords: Mie scattering, mid-infrared, anomalous dispersion, refractive index
PACC: 5225P, 7820, 7830G

1. Introduction

The study of light scattering and its applications is an enormous field.[1−8] For about a hundred years, Mie scattering theory, which is applied mainly to scattering and absorption by a spherical scatterer in air and other background materials (matrices), has been verified to a great extent, especially for visible light and microwaves.[9,10] In recent years, because of high-speed computers, Mie scattering calculations, related to anomalously dispersive materials, especially in the field of ultraviolet and ultrasonic properties, have become easy.[11,12] Since mid-infrared (mid-IR) radiation is usually regarded as an interest in military, medical, industrial or molecular spectroscopic fields, and techniques for detection of mid-IR rays are not so easy and sensitive as those for microwaves and visible light, the scattering by an anomalously dispersive scatterer in the mid-IR region has not been well studied.

In fact, investigations of Mie scattering in the mid-IR region will be very fruitful and interesting just as they were in the visible and microwave regions, because: (1) The wavelength of mid-IR radiation is longer than that of visible light, but only about one order of magnitude longer; therefore, a mid-IR sample of macroscopic-to-mesoscopic size would be suitable for practical applications in daily life. (2) There are many mid-IR-transparent materials which can be used as loss-free matrices, such as NaF, KBr, KCl, AgBr, liquid nujol, etc, whose refractive indices are between 1.3 and 2. Also, many of them have wide transparency regions up to ultraviolet, and can be pressed into pellets by manual operations.[13] (3) There are many mid-IR materials with high refractive indices, such as Ge (4.0), PbS (4.1), PbSe (4.7), PbTe (5.6), Te (4.7 for o-rays and 6.2 for e-rays) [14] and Bi_2Te_3 (9.2) [15,16] in the mid-IR range. (4) There are many anomalously dispersive dielectrics (ADD), such as SiC, MgO, and GeO_2, etc, each of which has a high-reflective reststrahlen band of its own. (5) The developments of mid-IR tunable short-pulse laser sources based on nonlinear optical principles and free electron lasers are advancing at a seemingly miraculous pace.[17−19]

In this paper, we report a theoretical investigation of refractive-index effects of matrices on the scattering and extinction efficiencies in the mid-IR region of the electromagnetic spectrum for three kinds of scattering systems, corresponding to an IR-transparent matrix inside which there is a high refractive index scatterer, an anomalously dispersive dielectric scatterer or

*Project supported by the State Key Development Program for Basic Research of China (Grant No 2001CB610402) and the National Natural Science Foundation of China (Grant No 1989380).

a metal scatterer. We hope our results and discussions promote the theoretical, experimental and applied research in Mie scattering in the mid-IR region.

2. Theoretical frame

For a single scattering problem, Mie scattering theory describes the scattering efficiency $Q_{\rm sca}$ and extinction efficiency $Q_{\rm ext}$ of a spherical scatterer as [13]

$$Q_{\rm sca} = \frac{1}{x^2}\sum_{\nu=1}^{\infty} 2(2\nu+1)(|a_\nu|^2+|b_\nu|^2) \qquad (1)$$

and

$$Q_{\rm ext} = \frac{1}{x^2}\sum_{\nu=1}^{\infty} 2(2\nu+1){\rm Re}\{a_\nu+b_\nu\}, \qquad (2)$$

where both the scattering efficiency $Q_{\rm sca}$ and extinction efficiency $Q_{\rm ext}$ depend on the complex refractive index of the scatterer relative to that of the background material (the matrix),

$$\hat{m} \equiv \hat{N}/n_0 = (n+{\rm i}n')/n_0 = m'+{\rm i}m'', \qquad (3)$$

and on the dimensionless size parameter x through the definition $x = 2\pi n_0 R/\lambda$ ($\hat{R}$ and n_0 are the refractive indices of the scatterer and the matrix respectively; R is the radius of the spherical scatterer, and λ is the radiation wavelength in a vacuum), a_ν and b_ν are Mie coefficients,

$$a_\nu = \frac{\hat{m}\psi_\nu(\hat{m}x)\psi'_\nu(x) - \psi_\nu(x)\psi'_\nu(\hat{m}x)}{\hat{m}\psi_\nu(\hat{m}x)\xi'_\nu(x) - \xi_\nu(x)\psi'_\nu(\hat{m}x)}, \qquad (4)$$

$$b_\nu = \frac{\hat{m}\psi_\nu(x)\psi'_\nu(\hat{m}x) - \psi_\nu(\hat{m}x)\psi'_\nu(x)}{\hat{m}\xi_\nu(x)\psi'_\nu(\hat{m}x) - \psi_\nu(\hat{m}x)\xi'_\nu(x)}. \qquad (5)$$

Here, ψ_ν and ξ_ν are the Riccati–Bessel functions, which are related to the half-integral Bessel functions of the first and second kinds, the spherical Bessel functions, and the third kind of Bessel function.[13]

If the matrix with refractive index $n_0 \neq 1$ is taken into account, which is the usual and practical case, the results will be qualitatively very different for the three kinds of scattering systems because their scattering mechanisms are very different from each other.

3. Refractive-index effects of matrices

3.1. Lossless scatterer

For the scattering system with a lossless scatterer, due to the fact that $\hat{m}$ is real (written simply as m in this case) to make $Q_{\rm sca}$=$Q_{\rm ext}$, both the scattering and extinction efficiencies can be written as Q. Figure 1 shows the calculated result of scattering (extinction) efficiency Q against x and m in the first few Mie resonant regions for a scatterer with $2.7 < m < 6.2$. Here, only the values larger than 7, which is approximately the peak value of the first Mie resonance of TiO_2 particle (n=2.73), are depicted. It can be seen from Fig.1 that the larger the m, the higher the first peak value of scattering (extinction) efficiency is. For example, for the scattering system with m=6.2, which corresponds to the case of Te (n=6.2) in air (n_0=1) or Bi_2Te_3 (n=9.2) in KBr (n_0=1.5), Q may be as large as 18, and meanwhile when m=3.1, which corresponds to InP (n=3.1) in air (n_0=1.0) or Ge (n=4.0) in NaF (n_0=1.32), the maximum Q decreases to 8.5. Therefore, for the first kind of scattering system, whose matrix and scatterers have a real constant refractive index, it is obvious that the introduction of the non-air matrix with refractive index larger than 1 may decrease the relative refractive index of the system while reducing the scattering efficiency—a behaviour that contrasts sharply with the second and third kinds of scattering systems, as we shall see.

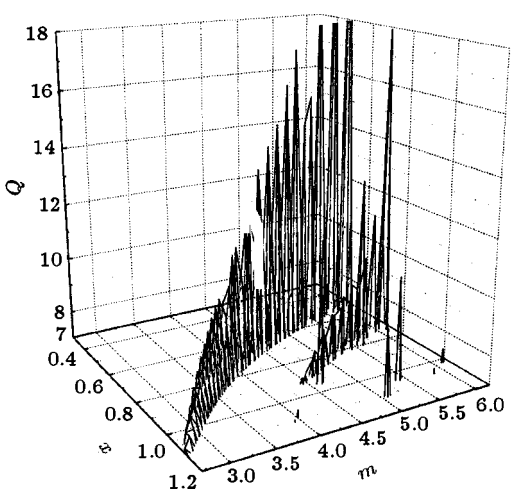


Fig.1. Q ($\geq$7) as a function of x and m in the lossless system.

3.2. Anomalously dispersive dielectric scatterer

For convenience in considering the second kind of scattering system, we define a system with a one-oscillator material α-SiC sphere as the scatterer. The α-SiC sphere[20] is regarded as a good "textbook" example, accurately described by the Lorentz dispersive model. Its complex dielectric function $\hat{\varepsilon}(\omega) = \varepsilon + {\rm i}\varepsilon' \equiv \hat{N}^2$ can be expressed as:[13]

$$\hat{\varepsilon}(\omega) = 6.7 + \frac{3.3\times 793^2}{793^2 - \omega^2 - {\rm i}4.76\omega}. \qquad (6)$$

Here, by the conventions of IR physics, the unit of radiation frequency ω is wavenumbers: cm^{-1}. The frequency dependence of the real part n and the imaginary part n' of the complex refractive index of α-SiC are shown schematically in Fig.2(a) in our chosen mid-IR region of 400–1200 cm^{-1}; meanwhile Fig.2(b) shows the normal incidence reflectance of α-SiC in the same region. From Fig.2, it can be seen that for bulk α-SiC in the region between about 800 and 970 cm^{-1} (the reststrahlen band[14]), where n is very small and n' is relatively large, the normal incident reflectance is as high as nearly 97%. Therefore, we expect that both of $Q_{sca} \geq 7$ and $Q_{ext} \geq 7$ occur in their own reststrahlen band.

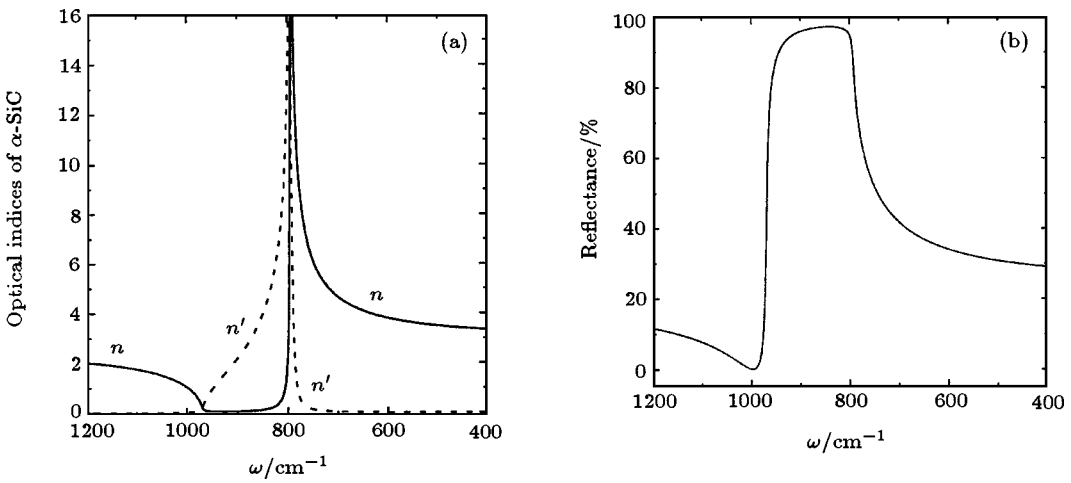


Fig.2. Optical indices (a) and reflectivity of normal incidence (b) of α-SiC in the mid-IR region of 400–1200 cm^{-1}.

Similar to the first kind of scattering system, Fig.3 shows the dependence of Q_{sca} and Q_{ext} plotted as a function of x and ω for an α-SiC particle in air. Also, for the convenience of comparison, only the values of Q_{sca} (Q_{ext}) ≥ 7 are shown. From Fig.3 it can be seen that both Q_{sca} and Q_{ext} may really be larger than 7 only in the 898–928 cm^{-1} and 895–935 cm^{-1} parts of the reststrahlen band, respectively. But neither can exceed 7 in the large-n region of 760–800 cm^{-1} because n' cannot be ignored. Moreover, if the matrix with $n_0 \neq 1$ is taken into account, the results will be very different from those obtained from the first kind of medium. Q_{sca} is plotted as a function of ω by an α-SiC particle in NaF (n_0=1.32) and in NaCl (n_0=1.56) in Fig.4(a) and (b), respectively. From Figs 3(a) and 4, one can see that the maximum value of Q_{sca} is about 10.4 for the air-matrix, about 11.5 for the NaF-matrix, and about 12.1 for the NaCl-matrix; and the region of $Q_{sca} \geq 7$ is 898–928 cm^{-1} for the air-matrix, 874–908 cm^{-1} for the NaF-matrix, and 860–896 cm^{-1} for the NaCl-matrix. Meanwhile, the width of the region of $Q_{sca} \geq 7$ is 30 cm^{-1} for the air-matrix, 34 cm^{-1} for the NaF-matrix, and 36 cm^{-1} for the NaCl-matrix.

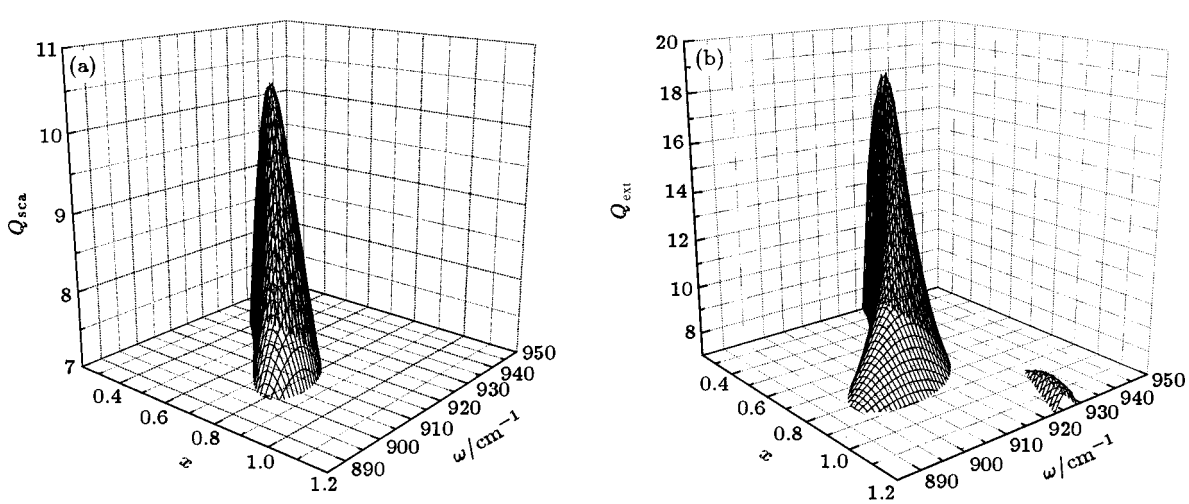


Fig.3. Dependence of Q_{sca} (a) and Q_{ext} (b) on x and ω for α-SiC particle in air.

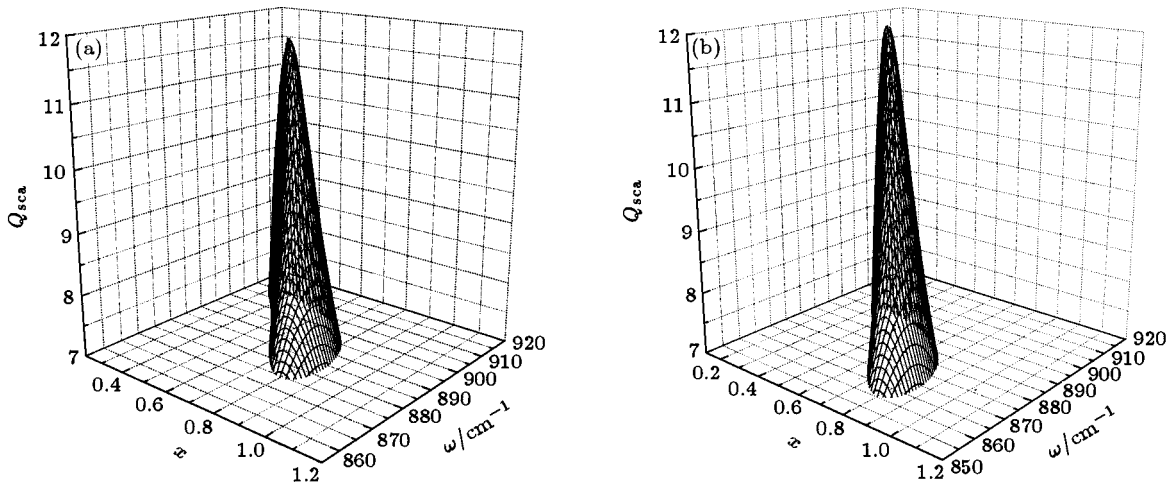


Fig.4. Q_{sca} as a function of ω by an α-SiC particle in NaF (n_0=1.32) (a) and in NaCl (n_0=1.56) (b).

To explain these, we should know that for bulk α-SiC in the reststrahlen band, the normal incident reflectance is as high as 97% because of small $n(\ll 1)$; i.e., "less than unity of the refractive index" in the field of infrared-energy-transmitting fibres—for example, n=0.06, n'=1.13 at the frequency of ω=943 cm^{-1}. Taking advantage of "less than unity of the refractive index" of some mid-IR ADD materials in their reststrahlen bands, the air (vacuum), which is lossless and has a refractive index of unity, becomes an optically denser medium,[21] and fibres transmitting CO_2 laser with high power have been fabricated using GeO_2 and Al_2O_3 in our group and in America, separately.[22,23] The larger the refractive index of the optically denser medium, the higher the reflectance is. Being mid-IR-transparent matrices, NaF and NaCl have the refractive indices of 1.32 and 1.56, respectively. Therefore, in order to obtain a higher scattering peak value, the former (NaF) is more suitable to serve as a matrix of the first kind of scattering system, whereas the latter (NaCl) is better to serve as a matrix of the second kind.

However, the circumstances are not so simple. When we increase n_0, the maximum value of Q_{sca} saturates immediately at 12.2 when n_0 is larger than 1.6, and then decreases with increasing n_0; that is, about 11.8 for the NaI-matrix (n_0=1.73), about 11.7 for the AgCl-matrix (n_0=2.0), about 11.1 for the ZnSe-matrix (n_0=2.43), and about 9.56 for the InP-matrix (n_0=3.1). Still, the region of high scattering efficiency tends to redshift in the smaller wavenumbers direction. This can be understood by considering that when the refractive index of the matrix is high, the imaginary part m'' of the relative refractive index $\hat{m}$ becomes insufficiently large (may be much less than 1).

We find, for the first time to the best of our knowledge, that the matrix plays an unusual role in the second kind of scattering system. It might enhance the scattering efficiency in some region of lower refractive index of the matrix, but not in some region of higher refractive index of the matrix. However, the region of high scattering efficiency and extinction efficiency redshifts regardless of the refractive index of the matrix. It may be concluded that α-SiC reflects the common properties of most of the ADD scatterers.

3.3. Metal scatterer

Optical properties of electrical conductors and nonconductors are markedly different, because the large number of free electrons in a conductor permits a small applied electric field to excite the nearly free electrons near the Fermi level into adjacent unoccupied states. Also, optical properties differ significantly among conductors in the regions of ultraviolet, visible and infrared. For example, silver is white, whereas copper is of a reddish-brown colour. However, for mid-IR and far-IR radiation, the Drude model obtained from the Lorentz model with ω_0=0 is accurate enough, and the dielectric function for a conductor (metal) is[13]

$$\hat{\varepsilon}(\omega) = 1 - \frac{\omega_p^2}{\omega^2 + i\gamma\omega}. \tag{7}$$

Here, γ is the damping constant of a near-free electron, ω_p is the plasma oscillation frequency. For most metals, $\hbar\omega_p$ is between 3 and 20 eV, and the corre-

sponding wavelength is less than 0.4 μm, or equivalently, the wavenumbers are greater than 25000 cm^{-1}. At room temperature, $\gamma \ll \omega_p$, and $\hbar\gamma$ is less than 1 eV, which corresponds to the frequency in the infrared. For aluminium $\hbar\omega_p$ is 12.7 eV, $\hbar\gamma$ is 0.13 eV (or ω_p is 1.01×10^5 cm^{-1}) and γ is 1050 cm^{-1}, so the dielectric function is[11]

$$\hat{\varepsilon}(\omega) = 1 - \frac{1.02 \times 10^{10}}{\omega^2 + 1050\mathrm{i}\omega}. \tag{8}$$

In the mid-IR region, the optical properties of metals are as follows: the real part ε of the dielectric function is large and negative, the imaginary part ε' is also large but positive, and the magnitude of both increases monotonically with increasing wavelength. In other words, the corresponding n and n' are both large at low frequencies and increase for longer wavelengths, and n' is greater than n. Therefore, normal incidence reflectance is always as high as 98%, or may be nearly 100% if we consider the grazing incidence, and even thin films would transmit little IR radiation.

Our third kind of scattering system uses metal spheres as a scatterer and mid-IR-transparent dielectric as the matrix material. Because both the bulk and thin film of a metal are highly reflective for mid-IR radiation, it is guessed that the albedo of a metal sphere is very high in the mid-IR region, i.e. $Q_{sca} \approx Q_{ext}$, indicating that the system is weakly absorptive. For three typical metals—aluminium (Al), silver (Ag) and iron (Fe)—we have evaluated the area scattering efficiencies Q_{sca} versus x in air, as shown in Fig.5. When evaluating, the following optical constants $\hat{N} = n+in'$ are used: 33+77i for aluminium, 14+54i for silver, and 6+31i for iron.[14] From Fig.5, we can see that scattering efficiency curves are similar to each other although n and n' of these three metals are significantly different from each other, which demonstrates that the scattering is independent of the relative complex refractive index m of the scatterer.

We have also evaluated the area scattering efficiency Q_{sca} of the typical metal aluminium (Al) as a function of x in air (n_0=1), NaF (n_0=1.32), and NaI (n_0=1.73) when ω=1000 cm^{-1}, as shown in Fig.6. It can be seen from Fig.6 that Q_{sca} arrives at its maximum value 2.5 near x=1. From Fig.6, it can be seen that Q_{sca} changes little although it increases slightly with increasing n_0. Therefore, we can say that the scattering efficiency is almost independent of the refractive index of the general matrix in the mid-IR region.

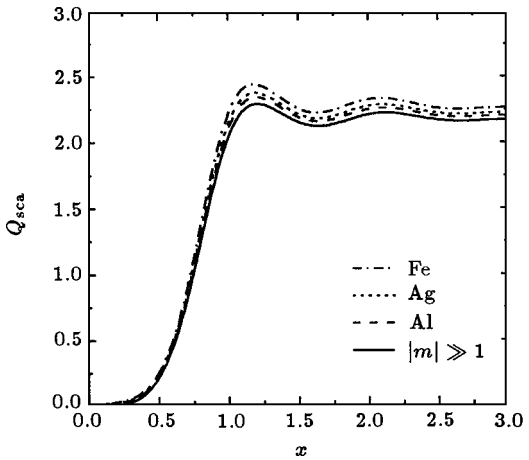


Fig.5. Q_{sca} by a Fe particle, an Ag particle, and an Al particle when ω=1000 cm^{-1} and by a particle with $|m| \gg 1$.

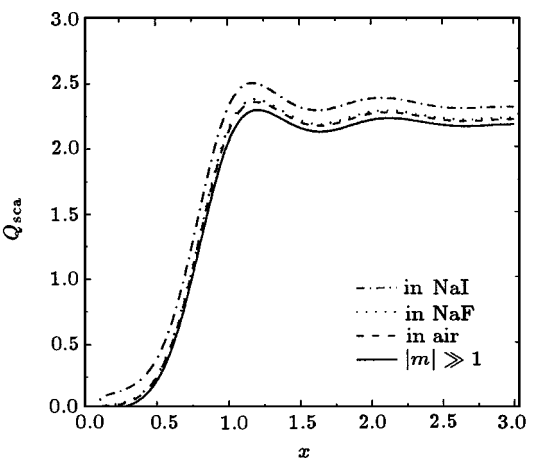


Fig.6. Q_{sca} by an Al particle in air (n_0=1), NaF (n_0=1.32), NaI (n_0=1.73) when ω=1000 cm^{-1} and by a particle with $|m| \gg 1$.

Thus, this can be considered to be a weak scattering system, contrary to our intuitive expectation for metal scatterers. This kind of scattering has a common property: the real part n and imaginary part n' of the complex refractive index $\hat{N}$ of the scatterer are very large throughout the mid-IR region, e.g., $|m| \gg 1$. Therefore, one can simplify the equations of Mie coefficients a_ν and b_ν using $|m| \gg 1$ to obtain a result without m

$$a_\nu = \frac{\psi'_\nu(x)}{\xi'_\nu(x)}, \tag{9}$$

$$b_\nu = \frac{\psi_\nu(x)}{\xi_\nu(x)}. \tag{10}$$

So the resulting Q_{sca} will denote all the scattering efficiencies of metal spheres shown as the solid curve in both Figs.5 and 6. From Figs.5 and 6, it can be

seen that our approximation is reasonable, and it is demonstrated that the scattering behaviours are quite similar for spheres of all the metals and in general matrices in the mid-IR region. The area scattering efficiency $Q_{\rm sca}$ is less than 2.5, meaning that the metal sphere is a kind of scatterer that has a low scattering efficiency and a large albedo. As the size of the metal scatterers discussed here is of the same order as the wavelength, this approximation is a new type of scattering which is different from other ones, such as Rayleigh scattering (small spheres $R \ll \lambda$, not too dense $x \ll 1$), Rayleigh–Gans scattering (low optical density $|\hat{N} - n_0| \ll 1$, not too large $|\hat{N} - n_0|x \ll 1$), small-dense-spheres scattering ($|m| \gg 1$, $x \ll 1$), van de Hulst scattering ($|\hat{N} - n_0| \ll 1$, $R \gg \lambda$), and geometrical-optics limit (large spheres $R \gg \lambda$, $x \gg 1$).[1]

As to the case of this metallic scatterer system in the mid-IR region, the limited refractive index of the matrix cannot affect the condition $|m| \gg 1$ significantly. Therefore, the role of the usual matrix is different here from that in both the first and second kinds of scattering systems, i.e., the usual matrix does not materially affect scattering efficiency in the third kind of scattering system.

4. Conclusion

We have applied a well-established theory to the study of the influence of a background material with a constantly high refractive index upon the scattering efficiency of (1) lossless scatterers, (2) anomalous dispersive dielectric scatterers and (3) metal scatterers in the mid-IR region of the electromagnetic spectrum. We have shown that although a background material with a higher refractive index reduces the scattering efficiency in the first kind of scattering system, it may or may not be conducive to scattering and extinguishing light in the second kind, and it has little effect on scattering and extinction efficiency in the third kind of scattering system. Therefore, we expect that this newly demonstrated effect of the matrix on Mie scattering in the mid-IR region will attract more attention and the application studies.

References

[1] Newton R G 1982 *Scattering Theory of Waves and Particles* (New York: Springer)
[2] Yao X C *et al* 2000 *Chin. Phys.* **9** 65
[3] Wang J G *et al* 2000 *Chin. Phys.* **9** 210
[4] Yao X C *et al* 2000 *Chin. Phys.* **9** 824
[5] Inami W and Kawata Y 2000 *Appl. Opt.* **39** 6369
[6] Tamaru H, Kuwata H, Miyazaki H T and Miyano K 2002 *J. Appl. Phys.* **80** 1826
[7] Liu X D *et al* 2002 *Acta Phys. Sin.* **51** 2117 (in Chinese)
[8] Liu X D *et al* 2002 *Acta Phys. Sin.* **51** 2123 (in Chinese)
[9] Swanson N L and Billard D B 2000 *Phys. Rev.* E **61** 4518
[10] Kushwaha M S *et al* 1998 *Eur. Phys. J.* B **3** 155
[11] Sujith R I *et al* 2001 *Exp. Fluids* **30** 339
[12] Felidj N, Aubard J and Levi G 1999 *J. Chem. Phys.* **111** 1195
[13] Bohren C F and Huffman D R 1983 *Absorption and Scattering of Light by Small Particles* (New York: Wiley)
[14] Bass M 1995 *Handbook of Optics* (Vol II) (New York: McGraw-Hill)
[15] Austin I G 1958 *Proc. Phys. Soc.* **72** 545
[16] Sehr R and Testardi L R 1962 *J. Phys. Chem. Solids* **23** 1219
[17] Rotermund F and Petrov V 2000 *Opt. Lett.* **25** 746
[18] Finsterbusch K, Urschel R and Zacharias H 2002 *Appl. Phys.* B **74** 319
[19] Xia J F, Song J and Strickland D 2002 *Opt. Commun.* **206** 149
[20] Spitzer W G, Kleinman D A and Wolsh D 1959 *Phys. Rev.* **113** 127
[21] Hidaka T, Morikawa T and Shimada J 1981 *J. Appl. Phys.* **52** 4467
[22] Hou L T *et al* 1997 *IR Phys. Tech.* **38** 193
[23] Harrington J A and Gregory C C 1990 *Opt. Lett.* **15** 541